Properties of DBD Plasma Jets using Powered Electrode With and Without Contact with the Plasma

Fellype do Nascimento, Konstantin Kostov, Munemasa Machida, Alexander Flacker

***Abstract*—An experimental investigation comparing the properties of plasma jets in dielectric barrier discharge (DBD) configurations using a powered electrode with and without a dielectric barrier, while keeping a second dielectric barrier over the grounded electrode, is reported in this work. For this purpose, two different power sources were used to produce the plasma jets, with one of them producing a pulsed high-voltage (HV) output and the other one producing a damped sine wave HV output, which acts as a pulse-like power source. Measurements of plasma parameters were performed for both configurations using argon and helium as working gases. As a result, if the pulsed power source is used, significant differences were found in discharge power (P_{dis}), rotational and vibrational temperatures (T_r and T_v, respectively) when switching from one configuration to the other. On the other hand, using the pulse-like HV only the P_{dis} parameter presented significant differences when switching the electrode's configuration. For the pulsed source it has been observed that despite the remarkable increase in P_{dis} when changing from the double barrier configuration to the single barrier one, the values obtained for T_r and T_v also increased, but not in the same proportion as the increase in P_{dis}, which suggests a non-linear dependency between temperatures and discharge power in the plasma jet. As an example for application of plasmas in both configurations, tests in an attempt to remove copper films deposited on alumina substrates were performed and, as a result, there was significant material removal only when the powered electrode was in contact with the plasma. As a general conclusion, if higher power is really required for applications that do not involve *in vivo* targets it is better to use this configuration.**

***Index Terms*—dielectric barrier discharge, DBD plasma, APPJ, plasma jets, plasma properties**

I. Introduction

PLASMA plumes produced under atmospheric pressure and in open environment generally referred to as Atmospheric Pressure Plasma Jets (APPJs) have been extensively studied in recent years, and a large number of applications for these devices have been developed due to their versatility, easy operation and low cost of implementation compared to low pressure plasmas [1], [2], [3], [4]. The APPJs applications can be in industry, biology and medicine, with the last field receiving great attention, especially due to successful treatments of cancerous tissues and, more recently, for combating viruses, including the Sars-Cov-2, and the success in biological treatments using APPJs is strongly related to the reactive oxygen and nitrogen species produced in such gas discharges [5], [6], [7], [8], [9], [10], [11], [12], [13], [14], [15], [16], [17]. Dielectric Barrier Discharge (DBD) is a kind of electrodes arrangement commonly employed to produce APPJs. Its main characteristic is the presence of at least one insulating layer between metallic plates [1], [3]. Among the various DBD configurations, the cylindrical geometry is the most commonly employed because it naturally takes advantage of using the gas flow to produce a plasma jet [2]. Even though many studies on different APPJ arrangements have been carried out, yet there is no a particular configuration that can be considered ideal, even for specific applications [3], [4]. Therefore, research goes on and different geometry configurations and device variations have been explored. It has been a considerable challenge to control plasma jet properties as well as to establish a relationship between different plasma parameters.

Among different electrode arrangements in cylindrical APPJ reactors, those setups that present powered electrodes at the center of the reactor have been commonly employed. They can have such electrode covered with a dielectric barrier, or not, that is, with the powered electrode in contact with the working gas or not. Each configuration will produce a plasma jet with different temperatures, power and/or density of reactive species that are created when the plasma interacts with the surrounding ambient air or with a surface [4], [18]. The first mentioned configuration (encapsulated powered electrode) presents higher electrical safety when compared to the other (a powered electrode without a dielectric barrier) and, for this reason, it is preferred for medical applications of plasma jets, especially when the treatments are *in vivo*.

Studies regarding the interaction between APPJs and different substrates have shown that the conductivity or dielectric properties of the substrate, as well as the distance from device output to the target surface, influence not only the treatment results, but can also modify the characteristics of the plasma jet itself [19], [20], [21], [22], [23], [24]. Works concerning differences in plasma jet properties when impinging on grounded or floating targets have been reported [25], [26]. To generate APPJs most devices use sinusoidal voltages, ranging in frequencies from kHz to MHz. Previous works of our group revealed that using conducting or dielectric targets (or sample holders) has important effect not only on plasma jet properties

F. Nascimento and K. Kostov are with the Faculty of Engineering, UNESP, Guaratingueta, SP, Brazil, emails: fellype@gmail.com, konstantin.kostov@unesp.br

M. Machida is with the Gleb Wataghin Physics Institute, UNICAMP, Campinas, SP, Brazil, email: machida@ifi.unicamp.br

A. Flacker is with the Renato Archer Center for Information Technology (CTI), Campinas, SP, Brazil, email: alexflacker@gmail.com

This work received financial support from CNPq and FAPESP

Accepted manuscript submitted March, 2021

but also on plasma treatment outcome [19], [27]. For instance it was verified that better adhesion of polydimethylsiloxane (PDMS) samples were achieved after plasma treatment using a conductive sample holder [27].

In this work we studied the behavior of three main parameters of an APPJ: rotational and vibrational temperatures (T_r and T_v, respectively) and mean discharge power (P_{dis}) in a DBD device in two distinct configurations. The first one employed is more often reported in the literature, in which a plasma jet is produced between two dielectric barriers, one enveloping the powered electrode and the other covering the grounded one. In the second configuration the dielectric on the powered electrode was partly removed while the one covering the grounded electrode was kept. This last configuration was not extensively explored yet, mainly due to safety issues appearing in medical applications of APPJs. Some works using microwave, sinusoidal and pulsed power sources have been reported using it but with no mention of measurements of plasma power, vibrational or rotational temperatures or comparison for different working gases [28], [29], [30], [31], [32], [33], [34], [35], [36]. Since some applications may not require the safe operating conditions provided by the dielectric barrier over the powered electrode, these can take advantage of the higher plasma power and other jet properties that can be achieved when the dielectric barrier is removed.

II. Materials and Methods

A schematic layout of the experimental setup is shown in Fig. 1. In order to produce the plasma jets using the pulsed power source, high voltage (HV) pulses of 20 kV amplitude and ∼250 ns width (at half peak voltage value) with positive polarity followed by a negative polarity pulse with -12 kV amplitude and ∼170 ns width, with 60 Hz repetition rate, were applied to a pin electrode covered with a glass tube with one of its ends closed (covered tip) or open (exposed tip), for the double and the single barrier configurations, respectively. Details about the pulsed power source can be found in [37]. A biaxially-oriented polyethylene terephthalate (BoPET) foil, 500 μm-thick and 10 cm-sided, was placed on the top of a grounded electrode and acted as a common dielectric barrier (the dielectric plate in Fig. 1) in both cases. The distance **d** between the end of the dielectric enclosure (a polyvinyl chloride tube) and the dielectric plate was kept constant and equal to 10 mm. Argon (Ar) and helium (He), both with 99.99% purity, were used as working gases at the same flow rate of 3.0 l/min. The damped sine wave power source consists of a HV supply whose output presents a damped sine waveform with an oscillation frequency of ∼150 kHz and 60 Hz repetition rate. This power source acts as a pulse-like one due to the small duration of the voltage waveform when compared to its repetition rate. The maximum positive voltage peak provided by this power source is ∼15 kV. The other parameters used in the experiment with the damped sine wave power source are the same as those mentioned for the pulsed one.

The light emitted by the plasma was collected using an optical fiber with 600 μm core diameter and numerical aperture of 0.22, providing an acceptance angle of 25.4°. The optical fiber was placed at the center of the plasma column, in both horizontal and vertical directions. The distance **L** between the end tip of the optical fiber and the center of plasma device was kept unchanged in all experiments and equal to 10 mm. The spectroscopic measurements were performed using a portable multi-channel spectrometer from OceanOptics (model HR4000), with a spectral resolution (full width at half maximum - FWHM) equal to (0.545 ± 0.007) nm, measured at 632.8 nm.

In order to obtain the rotational and vibrational temperatures of N_2 molecules, we use spectroscopic emissions from the N_2 second positive system, $C\,^3\Pi_u, \nu' \rightarrow B\,^3\Pi_g, \nu''$ (referred as $N_2(C \rightarrow B)$ hereafter), with $\Delta\nu = \nu' - \nu''$ = -2) in the wavelength range from 360 to 385 nm [38], [39], [40], [41]. Then comparisons between measured and simulated spectra are performed and the T_r and T_v pair of temperature values are determined by those that generate simulated curves that best fit to the experimental spectra, providing the lowest chi-squared value in the temperature ranges used to obtain the simulated curves. The spectral resolution value provided by the spectrometer is not enough to resolve rotational levels of the N_2 molecules and obtain accurate values for the T_r parameter. However, there is a direct relationship between the shape and broadening of the N_2 vibrational bands and the variation of the T_r values, being that the higher the T_r, the larger the broadening and also the higher the intensity of the rotational lines in the vibrational bands. Both effects cause a change in the shape of the vibrational bands in that part that degrades to violet, causing it to become higher and wider, allowing the estimation of the T_r values by using low-resolution spectrometers. Thus, even if not very accurate, the T_r values obtained can be good enough to show the trend of that parameter. The spectra simulations were performed using data from the SpecAir software [42]. We defined the uncertainties in the temperature measurements as:

$$\sigma T = \sqrt{(\Delta T/2)^2 + [(1 - R^2)T]^2} \quad (1)$$

where R^2 is the coefficient of determination obtained in the comparison between experimental and simulated spectra, T is the temperature value obtained for T_r or T_v, and ΔT is the temperature step used in the simulations, being that: for T_r, ΔT is 25 K, and for T_v, ΔT = 200 K. So, the uncertainty calculated using (1) takes into account both the temperature steps and the fittings quality when the experimental and simulated curves are compared.

The mean discharge power (P_{dis}) was calculated by measuring simultaneously the voltage applied on the powered electrode (point P_1 in the Fig. 1) and the voltage drop across a serial resistor R = 47 Ω (point P_2 of Fig. 1), which is used to calculate the current that flow through the plasma. In order to measure the applied voltage at P_1 a 1000:1 voltage probe (Tektronix model P6015A) was used, and the voltage measurement at P_2 was performed using a 100:1 voltage probe. The signals waveforms were recorded using a 100 MHz oscilloscope from Tektronix (model TBS1104B). Then, the P_{dis} value is obtained through the integration of

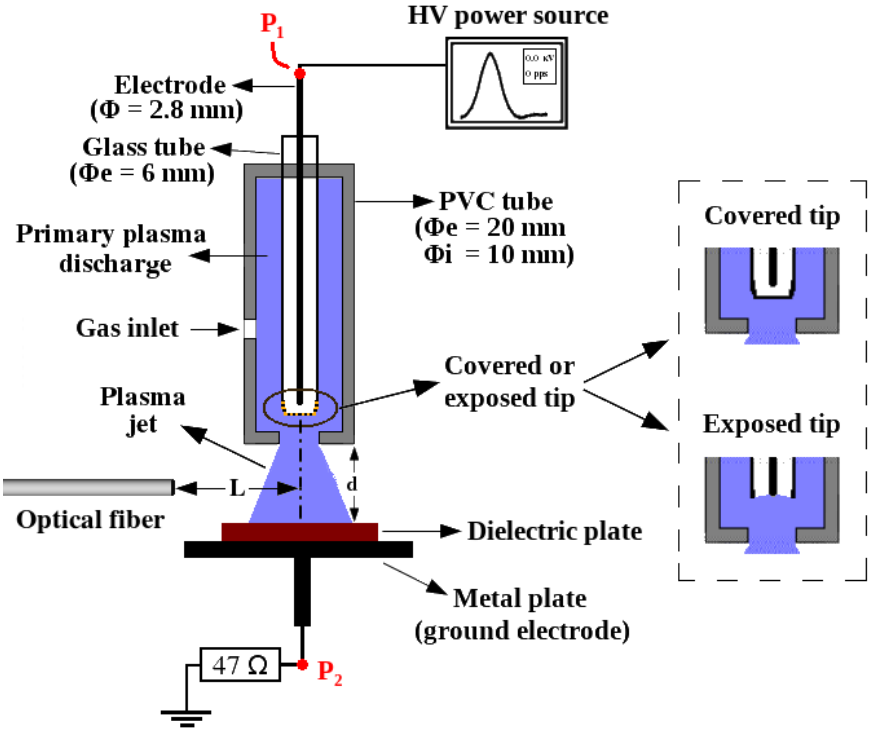

Fig. 1: Scheme used to produce the plasma jets in both configurations.

the product between voltage ($V(t)$) and current ($i(t)$) signals during the time of plasma pulse duration multiplied by the pulse repetition rate (f), that is [43], [44], [45], [46]:

$$P_{dis} = f \int_{t_1}^{t_2} V(t) i(t) dt \quad (2)$$

It is interesting to notice that $i(t)$ is composed by the discharge current itself and the displacement current in the gas gap [46].

Another important parameter that correlates optical measurements with an electrical quantity in APPJs is the reduced electric field strength $E_n = E/n$, where E is the electric field strength and n is the gas number density. The E_n value can be estimated using the ratio between intensity emissions from N_2^+ ions and excited N_2 ($I_{N_2^+}/I_{N_2}$), and variations in this ratio indicate change in E_n, being that the higher the ratio $I_{N_2^+}/I_{N_2}$, the higher the E_n value, that is $E_n \propto I_{N_2^+}/I_{N_2}$ [36], [47], [48]. The determination of E/n using the line ratio method may not consider quenching reactions for excited and ionized states of molecular nitrogen when noble gases containing metastable states with high energy levels, like helium and neon, are used as the working gas because in this case the Penning ionization reactions play a dominant role in the ionization and excitation processes in the plasma jet, making the quenching reactions be of less importance. Usually the emission from the first negative system of N_2^+ from the band ($B\,^2\Sigma_g+, \nu' = 0 \rightarrow X\,^2\Sigma_g^+, \nu'' = 0$), emitting at λ = 391.4 nm together with a $N_2(C \rightarrow B)$ emission coming from $N_2(C)$ energy level with ν' = 0 or 2 are used to calculate the $I_{N_2^+}/I_{N_2}$ ratio and obtain E_n. We choose using the $N_2(C, \nu' = 0 \rightarrow B, \nu'' = 2)$, emitting at λ = 380.49 nm to obtain I_{N_2} (referred as I_{380} hereafter) as well as the usual N_2^+ emission at λ = 391.4 nm to obtain $I_{N_2^+}$ (referred as I_{391} hereafter). However, the I_{391}/I_{380} ratios were not chosen to obtain E_n values in the APPJs in this work, but were only used to evaluate possible changes in plasma jet behaviors when switching from the double to the single barrier configuration.

In order to perform the tests attempting to remove copper (Cu) films deposited onto a 99.9% purity polished alumina (Al_2O_3) substrate, a 1 inch-sided square sample was used. The thickness of the Cu film is approximately 500 nm. The plasma application was performed statically, that is, the sample was positioned under the plasma jet and was not moved during the entire application time interval, which was equal to five minutes in each case. This part of the work was performed using only the pulsed power source to produce the plasma jets, since preliminary tests did not revealed significant removal of Cu film when using the damped sine wave power source.

III. Results

A. Electrical measurements

Figure 2 shows the current waveforms obtained using the pulsed source with Ar and He as working gases for (a) the double barrier configuration and (b) the single barrier one. Typical high-voltage (HV) waveforms obtained in each case, which have good repeatability, are also shown in Fig. 2. The values of the current measured in the single barrier configuration are notably higher, which is in agreement with what is expected to happen without an insulating barrier, justifying the choice of a double dielectric barrier configuration for applications that

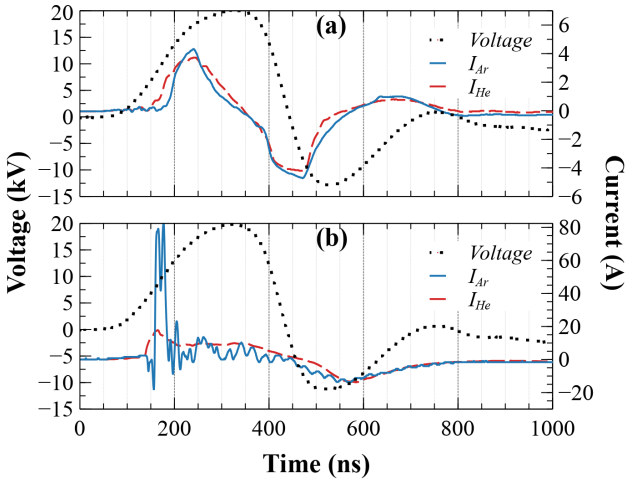

Fig. 2: Current and voltage waveforms measured in (a) double barrier configuration and (b) single barrier using the pulsed voltage source.

require electrical safety. The values obtained for the power in the double barrier configuration were 0.62 W when using Ar as the working gas, and 0.64 W when using He. For the single barrier configuration the power values were 2.98 W using Ar and 3.29 W using He. By changing the device configuration from double barrier to single barrier the P_{dis} values increased dramatically by approximately five times for both working gases, which is a great advantage for applications that require higher discharge power.

An interesting feature about the current waveforms shown in Fig. 2 is observed when operating in the double barrier configuration, the current signals for Ar and He gas (solid blue and dashed red curves, respectively) are almost equal, while in the single barrier configuration the current curves obtained for different gases do not behave in the same way, which suggests that different regimes are taking place depending on the working gas for the latter case. It can be also noticed that in the single barrier case, despite the P_{dis} values being close, the current signal measured with Ar (I_{Ar}) presents a very high peak value (∼80 A) at the beginning of the discharge, that is nearly four times higher than the peak value of the current obtained with He (I_{He}). Also, the temporal behavior of I_{Ar} is not as smooth as that observed for I_{He}, being that I_{Ar} presents a lot of oscillations as time evolves, which is another indication that the regime of the plasma jet using Ar as the working gas changes when the barrier over the powered electrode is removed. However, the same does not seem to happen when He is used as the working gas, which exhibits quite similar current behavior in both configurations.

In Fig. 2 we can also see that in the single barrier configuration the discharge currents start increasing earlier in the time interval between 100 and 150 ns, while using the double barrier the current peaks begin growing between 150 and 200 ns. In other words, as expected, lower voltage values are required to ignite the discharge in the single barrier case due to the powered electrode being in contact with the working gas and thus releasing more electrons from the metal to the

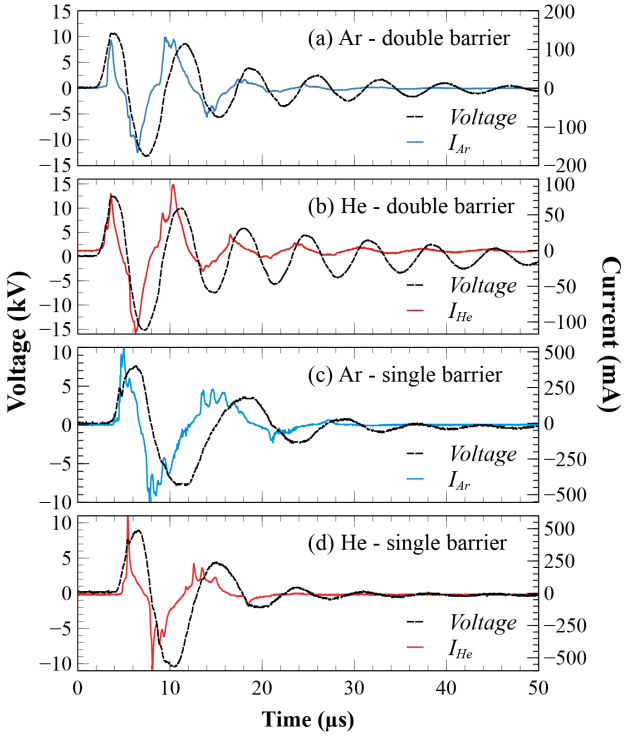

Fig. 3: Voltage and current waveforms measured using double barrier for Ar (a) and He (b), and using single barrier for Ar (c) and He (d) using the damped sine wave voltage source.

plasma. Moreover, when the first dielectric barrier is removed from the powered electrode the associated capacitance between the powered electrode and the discharge gap is removed too, and this also contributes to the early ignition of the plasma discharge. Those findings can also be the reasons for the more extended duration of the plasma discharge, depicted by the wider current pulses observed comparing figures 2 (a) and (b).

Figure 3 shows the voltage and current waveforms measured in double barrier configuration for Ar (a) and He (b), and in single barrier mode for Ar (c) and He (d) using the pulse-like voltage source. Notice that the time scales are in ns in Fig. 2 and in μs in Fig. 3. A point that is noteworthy when comparing double and single barrier configurations using the same gas (Ar or He) is that, unlike the pulsed power source, when the damped sine wave source is used significant voltage drops, from 10-12 kV to ∼8-9 kV for the first positive peaks, are observed when changing the configuration. The appearance of that voltage drop is due to the fact that the pulse-like source is more sensitive to the impedance matching. The change in the impedance caused by the removal of the first dielectric barrier results also in a change in the oscillating frequency of the damped sine wave power source from 150 kHz in the double barrier configuration to 110-120 kHz in the single one, as a consequence of the increase in the total capacitance of the system.

The values obtained for P_{dis} calculated using data presented in Fig. 3 were 0.27 W when using Ar as the working gas, and 0.23 W when using He in the double barrier configuration and

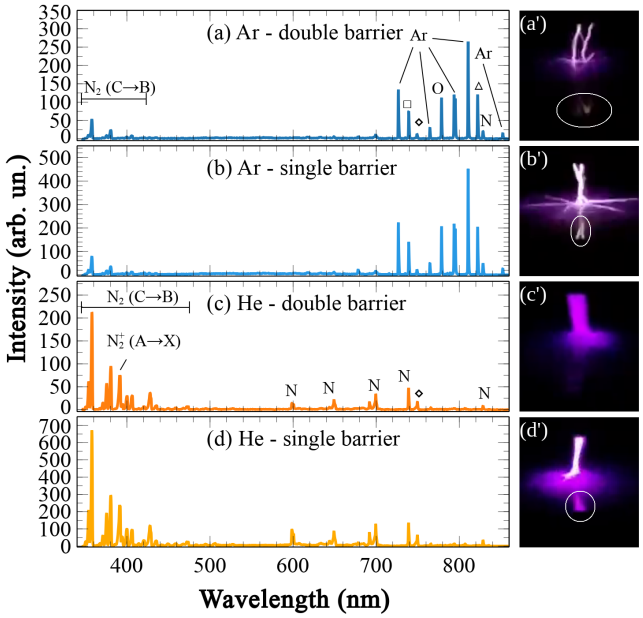

Fig. 4: Emission spectra obtained using the pulsed power source with argon as the working gas in (a) and (b) for the double and single barrier configurations, respectively, and the same for using helium in (c) and (d). (a′)-(d′) are the corresponding photos of plasma jets. The ellipses indicate reflections.

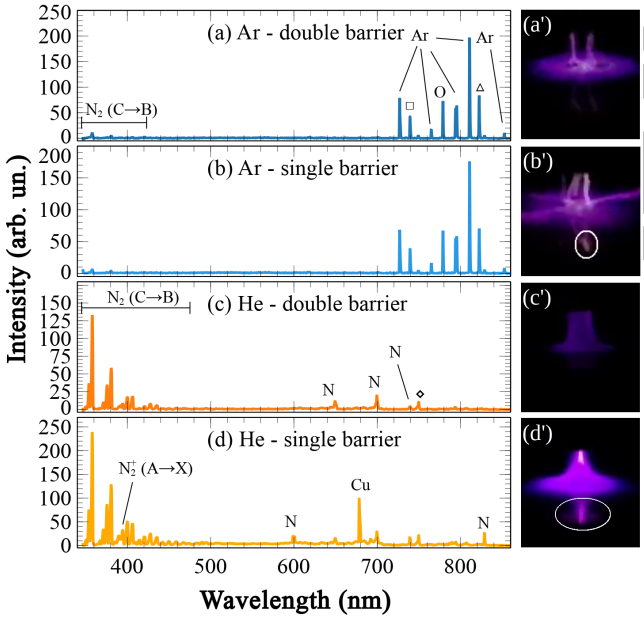

Fig. 5: Emission spectra obtained using the damped sine wave power source with argon as the working gas in (a) and (b) for the double and single barrier configurations, respectively, and the same for using helium in (c) and (d). (a′)-(d′) are the corresponding photos of plasma jets. The ellipses indicate reflections.

0.49 W using Ar and 0.48 W using He in the single barrier mode. Despite the voltage drop observed when changing the double barrier configuration to the single one, the observed values for the power increased in the second case. However, the increase was only ∼1.8 times using Ar and ∼2.1 times using He.

B. Spectroscopic measurements

An overview of the emission spectra in all conditions studied in this work is shown in Fig. 4, for the pulsed source, and in Fig. 5 for the damped sine wave one. All atomic emissions shown in Figs. 4 and 5 are from neutral species in excited states. Squares indicate superposed emissions from Ar and N, triangles indicate superposition of O and N lines and diamonds indicate an emission from the first positive system of N_2 $(B\ ^3\Pi, \nu' = 4 \rightarrow A\ ^3\Sigma, \nu'' = 2)$ [49]. The most intense atomic nitrogen lines come from multiplet systems and were observed at peak wavelengths 598.6 nm, 649.2 nm, 699.4 and 738.9 nm [50]. On the right side of Figs. 4 and 5 are also shown photos of the corresponding plasma jets produced in each configuration/working gas. The detailed views of the $N_2(C \rightarrow B)$ emission band used to calculate T_r and T_v are shown in Fig. 6 for the pulsed power source, and the results obtained for T_r and T_v using the pulse-like power source are shown in Table I.

Comparing the spectra in the Fig. 4 obtained in the case of pulsed source with double or single barriers for each gas, the noticeable differences are that the intensities of the atomic and molecular emissions are more intense when the plasma jet is operated using single dielectric barrier, which is in an agreement with the apparent higher luminosities shown in the corresponding photos. Furthermore, the change from double to single barrier plasma jet configuration do not result in any new excited species nor species emitting radiation in other wavelengths, that is, no new excitation levels were observed after the change. It is interesting to notice that the relative intensities of atomic species remain almost the same in the different configurations. However, even though there are no significant changes in the relative emissions intensities of different species, the fact that they have increased in absolute values when changing from the double barrier to the single barrier configuration indicates the production of more excited reactive species. This observation is associated to the higher discharge power values observed when using the single barrier configuration, which is also in agreement with studies reported on the literature [51], [52]. On the other hand, it was verified that the molecular species alone presented significant modifications in their relative intensities when keeping the same emission band (same $\Delta\nu$), and this results in significant changes on the T_v values, as can be seen in Fig. 6.

Contrary to what happened with the pulsed source when switching from the double to the single barrier configuration, when using the pulse-like power source it was observed an increase in the intensity of the emissions from atoms and molecules only when He was used as the working gas. An interesting observation can be made on the appearance of an emission line whose peak was detected at 678.29 nm in Fig. 5(d), which is possibly an emission from neutral Cu atoms (λ_{Ritz} = 677.57 nm) [50]. However, since there are

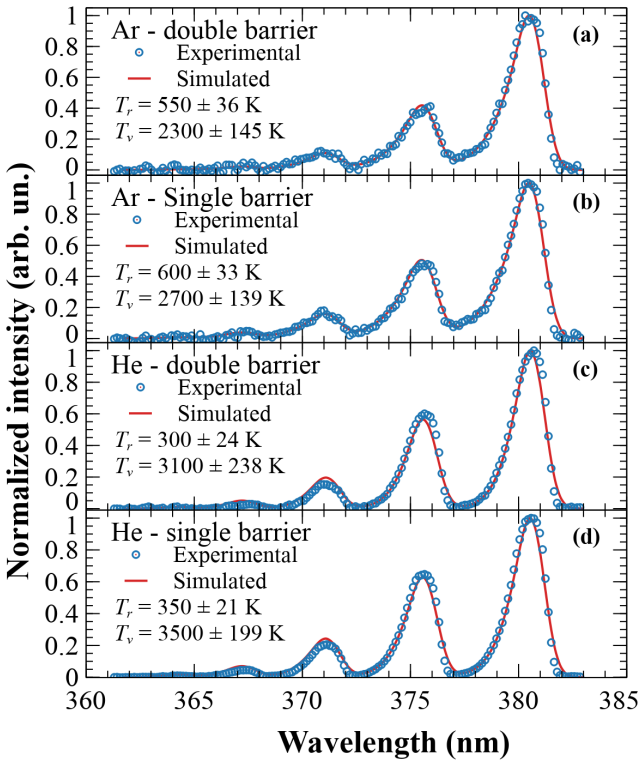

Fig. 6: Details of measured $N_2(C \rightarrow B)$ band emissions (circles) in the wavelength range from 360 to 385 nm and the respective simulated spectra (red lines) that best fit the experimental data using the pulsed power source.

no other line emissions from Cu in the observed spectrum, further investigation will be required in order to confirm this information.

From the spectra shown in Fig. 4, obtained from the plasmas produced using the pulsed power source, one can see that it is possible to calculate the I_{391}/I_{380} ratios only when He is used as the working gas because N_2^+ emissions are not present in the spectra obtained using Ar to generate the plasma jets. From Figs. 4(c) and 4(d), the I_{391}/I_{380} ratios for the double and single barrier configurations are 0.786 and 0.811, respectively, which corresponds to an increase of $\sim$3 % in the E_n value when switching from the double to the single barrier configuration. In other words, E_n remains almost constant when switching the device configuration, which means that the observed increase in the number of emitting species shown in Fig. 4 is mainly caused by the increase in the number of electrons released to the plasma, coming from the metallic electrode in contact with the plasma, which participate strongly in the ionization and excitation processes. Since E_n is almost constant when we switch from the double barrier configuration to the single one, it suggests that there are no changes in the operating plasma regime associated with the change in the device configuration when He is used as the working gas. It was not possible to perform the same analysis using the pulse-like power source due to the low intensity emission from the N_2^+ measured using the double barrier configuration.

From the photos shown in Figs. 4(a′-d′) and 5(a′)-(d′), one can notice that the plasma jets produced using the single barrier configuration tend to spread further on the impinged surface than those produced in the double barrier configuration (compare a′ with b′ and c′ with d′). These differences in the size of plasma jets spreading on the surface are related to the different electrical potentials (higher without the barrier on the powered electrode and smaller when the second dielectric barrier is used) that are being applied to the plasma in each condition. Therefore in the single barrier APPJ configuration, the potential difference between grounded electrode and the plasma is higher, producing higher current as well with a greater probability for the plasma plume to reach the target. From the photos Figs. 4(a′-d′) and 5(a′)-(d′) it can also be seen that the plasma jets are not homogeneous along the plasma column. So one can expect to observe some differences in the values of line intensity ratios, T_r and T_v when they are measured in different regions of the plasma column, specially when comparing the plasma channel region, where the spectroscopic measurements were performed, with the plasma located near the surface of the second dielectric barrier.

TABLE I: Rotational and vibrational temperatures obtained using the damped sine wave power source.

Parameter	T_r **(K)**		T_v **(K)**	
Working gas	*Ar*	*He*	*Ar*	*He*
Double barrier	500 ± 56	325 ± 73	1900 ± 217	3100 ± 549
Single barrier	500 ± 88	400 ± 62	1900 ± 337	3700 ± 573

From Fig. 6 we can see that when the pulsed power source is used both T_r and T_v values change when switching from the double barrier configuration to the single one, for both working gases used. Usually in APPJs the T_r value is considered to be very close to the gas temperature (T_{gas}) when the gas is in the plasma state, that is $T_r \approx T_{gas}$. Therefore regarding the obtained small variations in T_r values, 50 K for both gases, it is a good finding, since plasma jets as cold as possible are desirable in order to avoid possible thermal damages on samples subjected to APPJ treatment. In relation to the increment in T_v values for the single barrier plasma jet, 400 K for both gases, it is a very good result because one wants to produce APPJs with T_v values as high as possible due to the relationship between this parameter and chemical reaction rates. Thus plasma jets with higher T_v values are able to induce higher degree of surface activation [53], [54], [55].

On the other hand, as can be seen in table I the temperature variations obtained using the pulse-like source can not be considered significant since the uncertainties in the temperature values are higher than 15% of the measured ones in all cases. However, the increase in T_r and T_v values obtained using He when switching from the double to the single barrier configuration can be considered as a trend.

C. Applications on removal of copper films deposited onto alumina substrates

In order to verify some effects related to the choice of powered electrode covered or not with a dielectric material, we applied the plasma jets on a copper (Cu) film deposited

onto an alumina (Al_2O_3) surface using the pulsed power source. A consideration that should be taken into account before analyse the results is that the sample is a conducting material. So, it acts as a floating electrode when the plasma jet is applied to it and when using the powered electrode without the dielectric barrier, the discharge plasma regime can not be considered a DBD discharge, that is, the change in the target conductivity modifies drastically the nature of the discharge in the single barrier configuration. However, since the grounded electrode still covered with a dielectric, it is a valid experiment concerning the use of a powered electrode covered or not with a dielectric material. The sample used to perform the tests is shown in Fig. 7(a). Figure 7(b) shows the visual effects on the Cu film after applying plasma jets for five minutes for each of the configurations studied in the previous sections. The regions where the plasma jets were applied using Ar or He as working gases in double barrier (DB) or single barrier (SB) configurations are indicated in Fig. 7(c).

Comparing the photos in Figs. 7(a) and 7(b) it can be seen that evident visual effects are observed only when the single barrier configuration was used, operating with both Ar and He gases. The rounded marks in the sample, highlighted in blue in Fig. 7(b), correspond to the regions where there was significant removal of Cu film while in the regions highlighted in green, the removal of film was less significant. In preliminary tests we had found that the use of Ar in the single barrier configuration promoted greater removal of Cu films. Thus, we chose to apply plasma to the sample in the following order Ar-SB, He-SB, Ar-DB and He-DB. So, the possible effects of plasmas applied in one region to affect the other would favor greater removal of Cu film with less potent plasma conditions. However, this precaution is a redundancy, because when impinging the surface of the Cu film, the plasma does not spread through it as it would happen with an insulating target. The observed change in copper color before and after applying plasma is only due to the differences in lighting used to take the photos.

From Fig. 7(b) we can also verify that in the single barrier configuration the use of Ar as the working gas was able to remove the Cu film over an area larger than when using He. This result may be related to the higher peak current that occurs when using Ar.

IV. Discussion and conclusions

The experimental results obtained in this work using the pulsed power source are summarized in Table II, while the results obtained using the damped sine wave source are summarized in Table III.

Table II shows that the values of all measured parameters increase when changing from the double barrier configuration to the single one, using Ar or He as working gases. As can be seen in Table II, the T_r and T_v values presented differences not so far from the measurements uncertainties (especially for T_r). On the other hand, changing from double to single barrier configuration the P_{dis} values increased about 4.8 and 5.1 times when using Ar and He gases, respectively. This last result was expected because when the powered electrode is in contact with the working gas, a higher electric current will flow through the plasma jet, a result that is confirmed by the current waveforms measured for Ar and He using the double or the single barrier configurations.

TABLE II: Summarized results for the measured plasma temperatures and plasma power using the pulsed voltage.

Parameter	T_r **(K)**		T_v **(K)**		P_{dis} **(W)**	
Working gas	*Ar*	*He*	*Ar*	*He*	*Ar*	*He*
Double bar.	550±36	300±24	2300±145	3100±238	0.62	0.64
Single bar.	600±33	350±21	2700±139	3500±199	2.98	3.29

TABLE III: Summarized results for the measured plasma temperatures and plasma power using the damped sine wave voltage source.

Parameter	T_r **(K)**		T_v **(K)**		P_{dis} **(W)**	
Working gas	*Ar*	*He*	*Ar*	*He*	*Ar*	*He*
Double bar.	500±56	325±73	1900±217	3100±549	0.27	0.23
Single bar.	500±88	400±62	1900±337	3700±573	0.49	0.48

Concerning the different T_r and T_v values obtained in the two DBD configurations, one can conclude that it would be beneficial to use the single barrier one, since T_r does not change significantly while the T_v is higher compared to the double barrier case. However, due to the higher current and power values obtained for the single barrier jet, it is not readily suitable for applications that require electrical safety for the device operator or the target impinged by the plasma jet, as in *in vivo* applications. Besides that, the single barrier configuration combined with high voltage values is not suitable for applications on *in vivo* targets due to the risk of arc discharges between the high voltage electrode and the target. On the other hand, for this purpose high discharge power values can be achieved using the double barrier configuration by using pulsed power sources with higher pulse repetition rates. Nevertheless, the single barrier configuration is quite attractive for treatments of materials that require more powerful plasma to achieve an adequate degree of surface activation or higher interaction between the plasma and the target. An example of that is the application reported by Gazeli *et al* [26], where it was verified that a more powerful plasma jet is more efficient in the removal of resistant bibenzyl deposits formed on glass surfaces. In the present work, we have shown another example, verifying that the efficiency in the removal of a Cu film deposited onto an Al_2O_3 substrate was higher when more powerful plasma jets were used, noticing that the nature of the discharge has changed drastically due to the use of a conductive target.

Once the T_r and T_v values do not increase in the same proportion as P_{dis} increases when changing the DBD configuration, one can infer that there is no linear dependency between discharge power and the plasma jet temperatures, which is in agreement with some results reported in the literature [56]. However, to confirm or not this trend a further investigation is necessary. Besides, the possibility of plasma jets operating in different regime depending on the working gas for the single barrier case also needs to be investigated in more detail. In addition, studies using sinusoidal voltages instead of

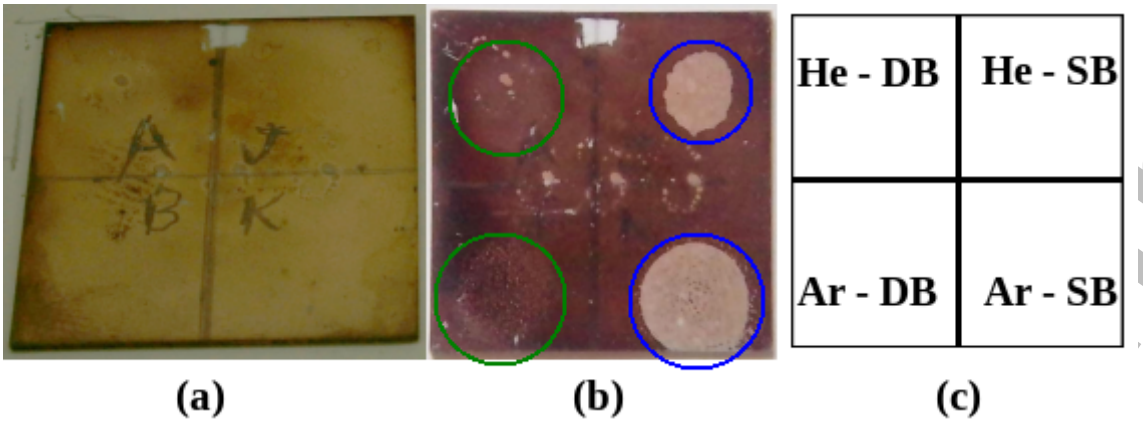

Fig. 7: Photos of a Cu film deposited onto Al_2O_3 substrate before (a) and after (b) plasma application using the pulsed power source. (c) Regions where plasma jets were applied using He and Ar in both configurations.

pulsed ones to produce the plasma jets should be performed in future experiments to complement the understanding of the differences in the plasma jet properties that occur when the device configurations are changed.

In Table III we can see that when the damped sine wave power source was used only the P_{dis} parameter changed significantly when switching the configuration from the double barrier to the single one. However, the observed increase in P_{dis} did not occur in the same proportion observed when using the pulsed source. This can be attributed partially to the voltage drop that occurred due to the change in electrode configuration and partially to the reduction of the observed frequency in the damped-sine waveform. Nevertheless, we can speculate that a pulsed voltage presents a more effective way for energy transfer from the power source to the plasma when operating in the single barrier mode.

ACKNOWLEDGMENT

F.N. thanks the Center for Semiconductor Components and Nanotechnologies (CCSNano/UNICAMP) for the loan of some equipments used in this work. This research received financial support from Brazilian National Council for Scientific and Technological Development (CNPQ) and from São Paulo Research Foundation (FAPESP) under grant #2020/09481-5.

REFERENCES

[1] U. Kogelschatz, "Dielectric-Barrier Discharges: Their History, Discharge Physics, and Industrial Applications," *Plasma Chemistry and Plasma Processing*, vol. 23, no. 1, pp. 1–46, Mar. 2003. [Online]. Available: https://doi.org/10.1023/A:1022470901385

[2] X. Lu, G. V. Naidis, M. Laroussi, and K. Ostrikov, "Guided ionization waves: Theory and experiments," *Physics Reports*, vol. 540, no. 3, pp. 123–166, Jul. 2014. [Online]. Available: http://www.sciencedirect.com/science/article/pii/S0370157314000441

[3] R. Brandenburg, "Dielectric barrier discharges: progress on plasma sources and on the understanding of regimes and single filaments," *Plasma Sources Sci. Technol.*, vol. 26, no. 5, p. 053001, Mar. 2017, publisher: IOP Publishing. [Online]. Available: https://doi.org/10.1088%2F1361-6595%2Faa6426

[4] X. Lu and K. K. Ostrikov, "Guided ionization waves: The physics of repeatability," *Applied Physics Reviews*, vol. 5, no. 3, p. 031102, Jul. 2018, publisher: American Institute of Physics. [Online]. Available: https://aip.scitation.org/doi/10.1063/1.5031445

[5] M. G. Kong, G. Kroesen, G. Morfill, T. Nosenko, T. Shimizu, J. v. Dijk, and J. L. Zimmermann, "Plasma medicine: an introductory review," *New J. Phys.*, vol. 11, no. 11, p. 115012, Nov. 2009, publisher: IOP Publishing. [Online]. Available: https://doi.org/10.1088/1367-2630/11/11/115012

[6] M. Vandamme, E. Robert, S. Pesnel, E. Barbosa, S. Dozias, J. Sobilo, S. Lerondel, A. L. Pape, and J.-M. Pouvesle, "Antitumor Effect of Plasma Treatment on U87 Glioma Xenografts: Preliminary Results," *Plasma Processes and Polymers*, vol. 7, no. 3-4, pp. 264–273, 2010, _eprint: https://onlinelibrary.wiley.com/doi/pdf/10.1002/ppap.200900080. [Online]. Available: https://onlinelibrary.wiley.com/doi/abs/10.1002/ppap.200900080

[7] J. Schlegel, J. Köritzer, and V. Boxhammer, "Plasma in cancer treatment," *Clinical Plasma Medicine*, vol. 1, no. 2, pp. 2–7, Dec. 2013. [Online]. Available: http://www.sciencedirect.com/science/article/pii/S2212816613000206

[8] S. Reuter, T. v. Woedtke, and K.-D. Weltmann, "The kINPen—a review on physics and chemistry of the atmospheric pressure plasma jet and its applications," *J. Phys. D: Appl. Phys.*, vol. 51, no. 23, p. 233001, May 2018, publisher: IOP Publishing. [Online]. Available: https://iopscience-iop.ez106.periodicos.capes.gov.br/article/10.1088/1361-6463/aab3ad/meta

[9] S. Bekeschus, P. Favia, E. Robert, and T. v. Woedtke, "White paper on plasma for medicine and hygiene: Future in plasma health sciences," *Plasma Processes and Polymers*, vol. 16, no. 1, p. 1800033, 2019, _eprint: https://onlinelibrary.wiley.com/doi/pdf/10.1002/ppap.201800033. [Online]. Available: https://onlinelibrary.wiley.com/doi/abs/10.1002/ppap.201800033

[10] A. Khlyustova, C. Labay, Z. Machala, M.-P. Ginebra, and C. Canal, "Important parameters in plasma jets for the production of RONS in liquids for plasma medicine: A brief review," *Front. Chem. Sci. Eng.*, vol. 13, no. 2, pp. 238–252, Jun. 2019. [Online]. Available: https://doi.org/10.1007/s11705-019-1801-8

[11] D. Braný, D. Dvorská, E. Halašová, and H. Škovierová, "Cold Atmospheric Plasma: A Powerful Tool for Modern Medicine," *International Journal of Molecular Sciences*, vol. 21, no. 8, p. 2932, Jan. 2020, number: 8 Publisher: Multidisciplinary Digital Publishing Institute. [Online]. Available: https://www.mdpi.com/1422-0067/21/8/2932

[12] A. Filipić, I. Gutierrez-Aguirre, G. Primc, M. Mozetič, and D. Dobnik, "Cold Plasma, a New Hope in the Field of Virus Inactivation," *Trends in Biotechnology*, Apr. 2020. [Online]. Available: http://www.sciencedirect.com/science/article/pii/S0167779920301086

[13] S. Bekeschus, A. Kramer, E. Suffredini, T. v. Woedtke, and V. Colombo, "Gas Plasma Technology—An Asset to Healthcare During Viral Pandemics Such as the COVID-19 Crisis?" *IEEE Transactions on Radiation and Plasma Medical Sciences*, vol. 4, no. 4, pp. 391–399, Jul. 2020, conference Name: IEEE Transactions on Radiation and Plasma Medical Sciences.

[14] G. Busco, E. Robert, N. Chettouh-Hammas, J.-M. Pouvesle, and C. Grillon, "The emerging potential of cold atmospheric plasma in skin

biology," *Free Radical Biology and Medicine*, vol. 161, pp. 290–304, Dec. 2020. [Online]. Available: http://www.sciencedirect.com/science/article/pii/S0891584920312776

[15] M. Laroussi, "Cold Plasma in Medicine and Healthcare: The New Frontier in Low Temperature Plasma Applications," *Front. Phys.*, vol. 8, 2020, publisher: Frontiers. [Online]. Available: https://www.frontiersin.org/articles/10.3389/fphy.2020.00074/full

[16] H. Cheng, J. Xu, X. Li, D. Liu, and X. Lu, "On the dose of plasma medicine: Equivalent total oxidation potential (ETOP)," *Physics of Plasmas*, vol. 27, no. 6, p. 063514, Jun. 2020, publisher: American Institute of Physics. [Online]. Available: https://aip.scitation.org/doi/10.1063/5.0008881

[17] Z. Chen, G. Garcia, V. Arumugaswami, and R. E. Wirz, "Cold atmospheric plasma for SARS-CoV-2 inactivation," *Physics of Fluids*, vol. 32, no. 11, p. 111702, Nov. 2020, publisher: American Institute of Physics. [Online]. Available: https://aip.scitation.org/doi/10.1063/5.0031332

[18] I. Adamovich, S. D. Baalrud, A. Bogaerts, P. J. Bruggeman, M. Cappelli, V. Colombo, U. Czarnetzki, U. Ebert, J. G. Eden, P. Favia, D. B. Graves, S. Hamaguchi, G. Hieftje, M. Hori, I. D. Kaganovich, U. Kortshagen, M. J. Kushner, N. J. Mason, S. Mazouffre, S. M. Thagard, H.-R. Metelmann, A. Mizuno, E. Moreau, A. B. Murphy, B. A. Niemira, G. S. Oehrlein, Z. L. Petrovic, L. C. Pitchford, Y.-K. Pu, S. Rauf, O. Sakai, S. Samukawa, S. Starikovskaia, J. Tennyson, K. Terashima, M. M. Turner, M. C. M. v. d. Sanden, and A. Vardelle, "The 2017 Plasma Roadmap: Low temperature plasma science and technology," *J. Phys. D: Appl. Phys.*, vol. 50, no. 32, p. 323001, Jul. 2017. [Online]. Available: https://doi.org/10.1088%2F1361-6463%2Faa76f5

[19] V. Prysiazhnyi, A. H. Ricci Castro, and K. G. Kostov, "Properties of Atmospheric Pressure Ar Plasma Jet Depending on Treated Dielectric Material," *Braz J Phys*, vol. 47, no. 1, pp. 65–71, Feb. 2017. [Online]. Available: https://doi.org/10.1007/s13538-016-0474-8

[20] D. Gidon, B. Curtis, J. A. Paulson, D. B. Graves, and A. Mesbah, "Model-Based Feedback Control of a kHz-Excited Atmospheric Pressure Plasma Jet," *IEEE Transactions on Radiation and Plasma Medical Sciences*, vol. 2, no. 2, pp. 129–137, Mar. 2018, conference Name: IEEE Transactions on Radiation and Plasma Medical Sciences.

[21] E. Simoncelli, A. Stancampiano, M. Boselli, M. Gherardi, and V. Colombo, "Experimental Investigation on the Influence of Target Physical Properties on an Impinging Plasma Jet," *Plasma*, vol. 2, no. 3, pp. 369–379, Sep. 2019, number: 3 Publisher: Multidisciplinary Digital Publishing Institute. [Online]. Available: https://www.mdpi.com/2571-6182/2/3/29

[22] E. A. Shershunova, S. I. Moshkunov, and V. Y. Khomich, "Features of Pulsed Argon Plasma Jet Impinging on Grounded Target," *IEEE Transactions on Plasma Science*, vol. 47, no. 11, pp. 4909–4914, Nov. 2019, conference Name: IEEE Transactions on Plasma Science.

[23] T. Teschner, R. Bansemer, K.-D. Weltmann, and T. Gerling, "Investigation of Power Transmission of a Helium Plasma Jet to Different Dielectric Targets Considering Operating Modes," *Plasma*, vol. 2, no. 3, pp. 348–359, Sep. 2019, number: 3 Publisher: Multidisciplinary Digital Publishing Institute. [Online]. Available: https://www.mdpi.com/2571-6182/2/3/27

[24] A. Stancampiano, T. Chung, S. Dozias, J. Pouvesle, L. M. Mir, and E. Robert, "Mimicking of Human Body Electrical Characteristic for Easier Translation of Plasma Biomedical Studies to Clinical Applications," *IEEE Transactions on Radiation and Plasma Medical Sciences*, vol. 4, no. 3, pp. 335–342, May 2020, conference Name: IEEE Transactions on Radiation and Plasma Medical Sciences.

[25] S. Bhatt, J. Pulpytel, S. Mori, M. Mirshahi, and F. Arefi-Khonsari, "Cell Repellent Coatings Developed by an Open Air Atmospheric Pressure Non-Equilibrium Argon Plasma Jet for Biomedical Applications," *Plasma Processes and Polymers*, vol. 11, no. 1, pp. 24–36, Jan. 2014. [Online]. Available: https://onlinelibrary-wiley.ez106.periodicos.capes.gov.br/doi/full/10.1002/ppap.201300076

[26] K. Gazeli, T. Vazquez, G. Bauville, N. Blin-simiand, B. Bournonville, S. PASQUIERS, and J. S. Sousa, "Experimental investigation of a ns-pulsed argon plasma jet for the fast desorption of weakly volatile organic compounds deposited on glass substrates at variable electric potential," *J. Phys. D: Appl. Phys.*, 2020. [Online]. Available: http://iopscience.iop.org/10.1088/1361-6463/aba870

[27] F. do Nascimento, S. Moshkalev, and M. Machida, "Changes in Properties of Dielectric Barrier Discharge Plasma Jets for Different Gases and for Insulating and Conducting Transfer Plates," *Braz J Phys*, vol. 47, no. 3, pp. 278–287, Jun. 2017. [Online]. Available: https://doi.org/10.1007/s13538-017-0492-1

[28] X. Lu, Z. Jiang, Q. Xiong, Z. Tang, and Y. Pan, "A single electrode room-temperature plasma jet device for biomedical applications," *Appl. Phys. Lett.*, vol. 92, no. 15, p. 151504, Apr. 2008, publisher: American Institute of Physics. [Online]. Available: https://aip.scitation.org/doi/abs/10.1063/1.2912524

[29] G.-D. Wei, C.-S. Ren, M.-Y. Qian, and Q.-Y. Nie, "Optical and Electrical Diagnostics of Cold Ar Atmospheric Pressure Plasma Jet Generated With a Simple DBD Configuration," *IEEE Transactions on Plasma Science*, vol. 39, no. 9, pp. 1842–1848, Sep. 2011, conference Name: IEEE Transactions on Plasma Science.

[30] A. F. H. v. Gessel, B. Hrycak, M. Jasiński, J. Mizeraczyk, J. J. A. M. v. d. Mullen, and P. J. Bruggeman, "Temperature and NO density measurements by LIF and OES on an atmospheric pressure plasma jet," *J. Phys. D: Appl. Phys.*, vol. 46, no. 9, p. 095201, Jan. 2013. [Online]. Available: https://doi.org/10.1088%2F0022-3727%2F46%2F9%2F095201

[31] W. V. Gaens and A. Bogaerts, "Reaction pathways of biomedically active species in an Ar plasma jet," *Plasma Sources Sci. Technol.*, vol. 23, no. 3, p. 035015, May 2014, publisher: IOP Publishing. [Online]. Available: https://doi.org/10.1088%2F0963-0252%2F23%2F3%2F035015

[32] E. Ilik and T. Akan, "Optical properties of the atmospheric pressure helium plasma jet generated by alternative current (a.c.) power supply," *Physics of Plasmas*, vol. 23, no. 5, p. 053501, May 2016, publisher: American Institute of Physics. [Online]. Available: https://aip.scitation.org/doi/abs/10.1063/1.4948718

[33] T. Darny, J.-M. Pouvesle, V. Puech, C. Douat, S. Dozias, and E. Robert, "Analysis of conductive target influence in plasma jet experiments through helium metastable and electric field measurements," *Plasma Sources Sci. Technol.*, vol. 26, no. 4, p. 045008, Mar. 2017, publisher: IOP Publishing. [Online]. Available: https://doi.org/10.1088%2F1361-6595%2Faa5b15

[34] G. D. Deepak, N. K. Joshi, D. K. Pal, and R. Prakash, "A low power miniaturized dielectric barrier discharge based atmospheric pressure plasma jet," *Review of Scientific Instruments*, vol. 88, no. 1, p. 013505, Jan. 2017, publisher: AIP Publishing LLC AIP Publishing. [Online]. Available: https://aip.scitation.org/doi/abs/10.1063/1.4974101

[35] J.-J. Qiao, L. Zhang, D.-Z. Yang, Z.-X. Jia, Y. Song, Z.-L. Zhao, H. Yuan, Y. Xia, and W.-C. Wang, "Temporal evolution of the relative vibrational population of N2 (C3$\prod$u) and optical emission spectra of atmospheric pressure plasma jets in He mixtures," *J. Phys. D: Appl. Phys.*, vol. 52, no. 28, p. 285203, May 2019, publisher: IOP Publishing. [Online]. Available: https://doi.org/10.1088%2F1361-6463%2Fab1110

[36] L. Zhang, D. Yang, S. Wang, Z. Jia, H. Yuan, Z. Zhao, and W. Wang, "Discharge Regimes Transition and Characteristics Evolution of Nanosecond Pulsed Dielectric Barrier Discharge," *Nanomaterials*, vol. 9, no. 10, p. 1381, Oct. 2019, number: 10 Publisher: Multidisciplinary Digital Publishing Institute. [Online]. Available: https://www.mdpi.com/2079-4991/9/10/1381

[37] M. Machida, "Ferrite Loaded DBD Plasma Device," *Braz J Phys*, vol. 45, no. 1, pp. 132–137, Feb. 2015. [Online]. Available: https://doi.org/10.1007/s13538-014-0293-8

[38] S. Y. Moon and W. Choe, "A comparative study of rotational temperatures using diatomic OH, O2 and N2+ molecular spectra emitted from atmospheric plasmas," *Spectrochimica Acta Part B: Atomic Spectroscopy*, vol. 58, no. 2, pp. 249–257, Feb. 2003. [Online]. Available: http://www.sciencedirect.com/science/article/pii/S0584854702002598

[39] P. J. Bruggeman, N. Sadeghi, D. C. Schram, and V. Linss, "Gas temperature determination from rotational lines in non-equilibrium plasmas: a review," *Plasma Sources Sci. Technol.*, vol. 23, no. 2, p. 023001, Apr. 2014. [Online]. Available: https://doi.org/10.1088%2F0963-0252%2F23%2F2%2F023001

[40] Q. Y. Zhang, D. Q. Shi, W. Xu, C. Y. Miao, C. Y. Ma, C. S. Ren, C. Zhang, and Z. Yi, "Determination of vibrational and rotational temperatures in highly constricted nitrogen plasmas by fitting the second positive system of N2 molecules," *AIP Advances*, vol. 5, no. 5, p. 057158, May 2015, publisher: American Institute of Physics. [Online]. Available: https://aip.scitation.org/doi/10.1063/1.4921916

[41] R. Ono, "Optical diagnostics of reactive species in atmospheric-pressure nonthermal plasma," *J. Phys. D: Appl. Phys.*, vol. 49, no. 8, p. 083001, Jan. 2016, publisher: IOP Publishing. [Online]. Available: https://doi.org/10.1088%2F0022-3727%2F49%2F8%2F083001

[42] SpecAir, "Website of SpecAir software, http://specair-radiation.net/ - last access in 7/29/2020," 2020. [Online]. Available: http://specair-radiation.net/

[43] M. Hołub, "On the measurement of plasma power in atmospheric pressure DBD plasma reactors," *International Journal of Applied Electromagnetics and Mechanics*,

vol. 39, no. 1-4, pp. 81–87, Jan. 2012, publisher: IOS Press. [Online]. Available: https://content.iospress.com/articles/international-journal-of-applied-electromagnetics-and-mechanics/jae01446

[44] D. E. Ashpis, M. C. Laun, and E. L. Griebeler, "Progress Toward Accurate Measurement of Dielectric Barrier Discharge Plasma Actuator Power," *AIAA Journal*, vol. 55, no. 7, pp. 2254–2268, 2017. [Online]. Available: https://doi.org/10.2514/1.J055816

[45] D. B. Nguyen, Q. H. Trinh, M. M. Hossain, W. G. Lee, and Y. S. Mok, "Improvement of Electrical Measurement of a Dielectric Barrier Discharge Plasma Jet," *IEEE Transactions on Plasma Science*, vol. 47, no. 5, pp. 2004–2010, May 2019, conference Name: IEEE Transactions on Plasma Science.

[46] A. V. Pipa and R. Brandenburg, "The Equivalent Circuit Approach for the Electrical Diagnostics of Dielectric Barrier Discharges: The Classical Theory and Recent Developments," *Atoms*, vol. 7, no. 1, p. 14, Mar. 2019, number: 1 Publisher: Multidisciplinary Digital Publishing Institute. [Online]. Available: https://www.mdpi.com/2218-2004/7/1/14

[47] P. Paris, M. Aints, F. Valk, T. Plank, A. Haljaste, K. V. Kozlov, and H.-E. Wagner, "Intensity ratio of spectral bands of nitrogen as a measure of electric field strength in plasmas," *J. Phys. D: Appl. Phys.*, vol. 38, no. 21, pp. 3894–3899, Oct. 2005. [Online]. Available: https://doi.org/10.1088%2F0022-3727%2F38%2F21%2F010

[48] A. Obrusník, P. Bílek, T. Hoder, M. Šimek, and Z. Bonaventura, "Electric field determination in air plasmas from intensity ratio of nitrogen spectral bands: I. Sensitivity analysis and uncertainty quantification of dominant processes," *Plasma Sources Sci. Technol.*, vol. 27, no. 8, p. 085013, Aug. 2018, publisher: IOP Publishing. [Online]. Available: https://doi.org/10.1088/1361-6595/aad663

[49] R. W. B. Pearse and A. G. Gaydon, *The identification of molecular spectra*, second edition, revised ed. London: Chapman and Hall Ltd, 1950.

[50] A. Kramida, Y. Ralchenko, J. Reader, and N. A. Team, "NIST Atomic Spectra Database (ver. 5.8), [Online]," 2021. [Online]. Available: https://physics.nist.gov/asd

[51] E. J. Baek, H. M. Joh, S. J. Kim, and T. H. Chung, "Effects of the electrical parameters and gas flow rate on the generation of reactive species in liquids exposed to atmospheric pressure plasma jets," *Physics of Plasmas*, vol. 23, no. 7, p. 073515, Jul. 2016, publisher: American Institute of Physics. [Online]. Available: https://aip.scitation.org/doi/abs/10.1063/1.4959174

[52] F. do Nascimento, M. Machida, K. G. Kostov, and S. Moshkalev, "Four-electrodes DBD plasma jet device with additional floating electrode," *Eur. Phys. J. D*, vol. 74, no. 1, p. 14, Jan. 2020. [Online]. Available: https://doi.org/10.1140/epjd/e2019-100343-9

[53] J. D. Lambert, "Vibration–vibration energy transfer in gaseous collisions," *Q. Rev. Chem. Soc.*, vol. 21, no. 1, pp. 67–78, Jan. 1967. [Online]. Available: https://pubs.rsc.org/en/content/articlelanding/1967/qr/qr9672100067

[54] R. R. Smith, D. R. Killelea, D. F. DelSesto, and A. L. Utz, "Preference for Vibrational over Translational Energy in a Gas-Surface Reaction," *Science*, vol. 304, no. 5673, pp. 992–995, May 2004. [Online]. Available: https://science.sciencemag.org/content/304/5673/992

[55] F. do Nascimento, M. Machida, M. A. Canesqui, and S. A. Moshkalev, "Comparison Between Conventional and Transferred DBD Plasma Jets for Processing of PDMS Surfaces," *IEEE Transactions on Plasma Science*, vol. 45, no. 3, pp. 346–355, Mar. 2017.

[56] S. Y. Moon, W. Choe, and B. K. Kang, "A uniform glow discharge plasma source at atmospheric pressure," *Appl. Phys. Lett.*, vol. 84, no. 2, pp. 188–190, Jan. 2004. [Online]. Available: https://aip.scitation.org/doi/10.1063/1.1639135

photo-fellype.jpg

Fellype do Nascimento received both the B.S. and the Ph.D. degree in physics from State University of Campinas, Campinas, Brazil, in 2006 and 2013, respectively. He was as a postdoctoral fellow at the Semiconductor Components Center at the State University of Campinas, from 2014 to 2018. He has experience in the field of Plasma Physics, with an emphasis on the development and use of diagnostics based on spectroscopy techniques, optical and electrical characterization of plasma jets produced under atmospheric pressure, in the treatment of material surfaces using plasmas generated by dielectric barrier discharge (DBD), and also in the development and characterization of devices for production of plasma jets at atmospheric pressure. He is currently a postdoctoral fellow at the Faculty of Engineering of Guaratinguetá (FEG/Unesp), working on the development and characterization of devices to generate plasma jets for applications in dentistry.

Konstantin Georgiev Kostov received the B.S. degree in physics and the Ph.D. degree in plasma physics from Sofia University, Sofia, Bulgaria, in 1984 and 1994, respectively.He was a Post-Doctoral Fellow with McMaster University, Hamilton, ON, Canada, from 1995 to 1996. From 1998 to 1999, he held a post-doctoral position with the Institute for Space Research, São Paulo, Brazil, where he was a Visiting Researcher from 2001 to 2003. In 2004, he joined the Department of Physics and Chemistry with the Faculty of Engineering of Guaratingueta, São Paulo State University, São Paulo. His current research interests include gas discharges, plasma immersion ion implantation, and atmospheric pressure plasmas, such as dielectric barrier discharges and cold plasma jets for material surface modification and decontamination.

Munemasa Machida was born in Japan in August 1950 and has resided in Brazil since 1961. He received the B.S. degree in physics from the University of São Paulo, São Paulo, Brazil, and the Ph.D. degree from Columbia University (APNE), New York, NY, in 1983. He was a Professor Collaborator with the Plasma Group, University of São Paulo, working on tokamak research and is currently with Plasma Physics Laboratory, Institute of Physics "Gleb Wataghin," Campinas State University, Campinas, Brazil. His research interests include plasma diagnostic techniques, building and operation of theta pinch, tokamak, pulsed plasma processing devices and atmospheric pressure plasma jets.

Alexander Flacker is Graduated in Chemistry at Faculdades Oswaldo Cruz (1975). Has experience in the area of Chemistry, mainly in Analytical Chemistry, Materials and Surface Treatment. He has experience in metallization of materials using vacuum, chemical and electrolytic processes, and also in optical fibers. His research interests include the following subjects: alumina, silicon, metallization, thin films, polymers and carbon nanotubes.